

RSC Advances

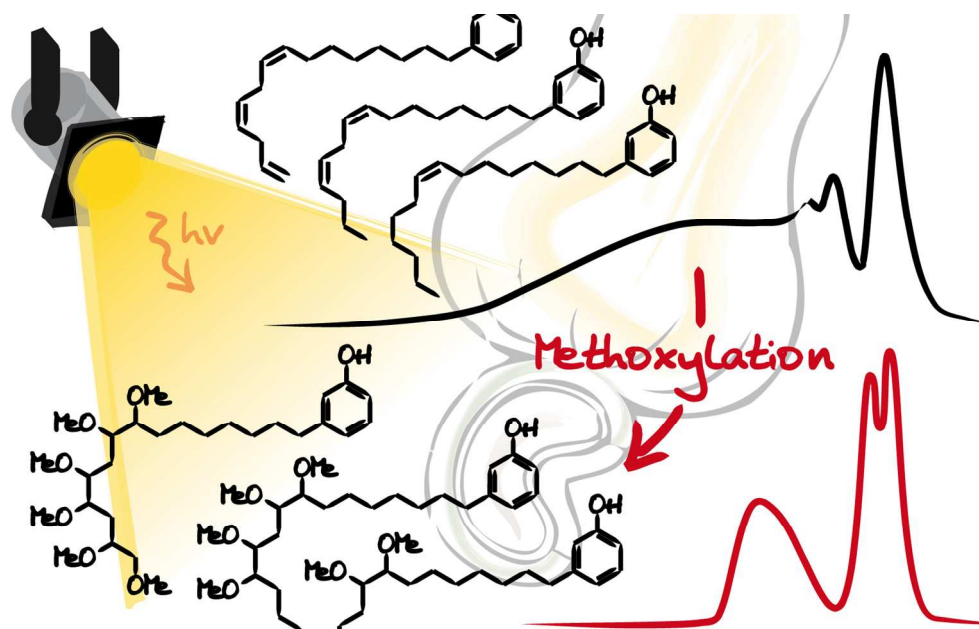


This is an *Accepted Manuscript*, which has been through the Royal Society of Chemistry peer review process and has been accepted for publication.

Accepted Manuscripts are published online shortly after acceptance, before technical editing, formatting and proof reading. Using this free service, authors can make their results available to the community, in citable form, before we publish the edited article. This *Accepted Manuscript* will be replaced by the edited, formatted and paginated article as soon as this is available.

You can find more information about *Accepted Manuscripts* in the [Information for Authors](#).

Please note that technical editing may introduce minor changes to the text and/or graphics, which may alter content. The journal's standard [Terms & Conditions](#) and the [Ethical guidelines](#) still apply. In no event shall the Royal Society of Chemistry be held responsible for any errors or omissions in this *Accepted Manuscript* or any consequences arising from the use of any information it contains.



photoaging of cardanol and its limitation by methoxylation of the side chain to produce photocrosslinkable copolymers of tunable reactivity
142x87mm (300 x 300 DPI)

ARTICLE

Photoageing of cardanol: characterization, circumvention by side chain methoxylation and application for photocrosslinkable polymers

Cite this: DOI: 10.1039/x0xx00000x

T. Fouquet, L. Fetzer, G. Mertz, L. Puchot and P. Verge

Received
Accepted

DOI: 10.1039/x0xx00000x

www.rsc.org/

The photosensitivity of cardanol has been evaluated using a multi-technique approach. Among others, size exclusion chromatography, matrix assisted laser desorption ionization mass spectrometry and their off line coupling provided useful details about the macroscopically observed yellowing and insolubility of cardanol under UV activation by analyzing photoproducts at the molecular level. Evidencing the implication of the unsaturations borne by the cardanol side chain in a crosslinking process, an original synthesis route leading to its complete methoxylation has been proposed as a way to lower the photosensitivity of cardanol. Using a similar set of analytical techniques, this newly synthesized methoxylated cardanol has appeared more resistant towards UV exposure, without any crosslinking but a simple dimerization preserving its solubility. As a direct application, copolymers made from methyl methacrylate, cardanol and methoxylated cardanol have been synthesized, and their photocrosslinking ability found to depend on the content of the two latter co-monomer, as a preliminary step towards the production of photocrosslinkable bio-based polymers with a tunable UV curing propensity.

Introduction

Cashew nutshell liquid (CNSL)¹ is an abundant annually renewable agricultural non-food by-product extracted from the honeycomb structure of cashew nutshells and forms the basic raw material for a vast number of industrially important chemicals and chemical intermediates,² such as antioxidants³ or plasticizers.⁴ A thermal treatment of CNSL permits the production of cardanol, a phenol derivative bearing a C15 polyunsaturated side chain in meta position,⁵ at industrial scale. Cardanol is actually composed of four components – namely tri-, di-, mono-unsaturated congeners and the saturated constituent (ESI† for their structures). This intrinsically reactive alkyl chain constitutes an interesting platform for chemical modifications and functionalizations.^{6,7} For instance, cardanol-grafted rubbers have been produced by its chemical grafting through the C15 side chain.^{8,9} From a structural point of view, a generic poly(butadiene) PB (unsaturations spaced by $-\text{CH}_2-\text{CH}_2-$, ESI†) could roughly mimic the feature of the side chain of cardanol (unsaturations spaced by $-\text{CH}_2-$). PB is notoriously sensitive to photoageing under either natural or accelerated UV irradiation^{10,11} through the abstraction of the hydrogen atoms in alpha position of the unsaturations, followed by oxidative processes ultimately leading to oligomerization and chain scission. The oligomerization route is of prime importance: taking the opposite view from *photoageing*, one could consider

PB as a *photocrosslinkable* substrate under mild UV activation, *ie* a property rather than a deleterious drawback. Similarly, and with a probably greater propensity to react owing to the vicinity of the double bonds, cardanol could thus be seen as a photocrosslinkable renewable chemical. Suresh et al have shown that a copolymer made of methyl methacrylate (MMA) and acrylated cardanol could be of interest to produce photocrosslinkable thin layers used as adhesives or inks.¹² A thorough understanding of the processes behind the expected photopolymerization of cardanol would be valuable to properly design photocrosslinkable chemicals or polymers. In addition, finding a way to limit such photo-crosslinking would allow a fine tuning of the photosensitivity of the resulting materials, broadening the scope of applications. This article thus offers a first exploration of the behavior of cardanol under UV irradiation, using a multi-technique analytical strategy combining Fourier transform infrared spectroscopy (FTIR), UV/Vis spectroscopy, size exclusion chromatography (SEC) and its coupling with mass spectrometry (MS) to gain more and more insights into the nature of the photoproducts issued from cardanol. A chemical modification of its side chain – namely methoxylation– will then be proposed as a way to circumvent an early photocrosslinking of cardanol by eliminating the reactive C=C functions. A similar set of analytical tools will be deployed to properly characterize this newly synthesized cardanol derivative and evaluate the reduction of its photosensitivity.

Finally, a direct application will be proposed through the synthesis of MMA/cardanol copolymer (similarly to those proposed by Suresh et al¹²), MMA/methoxylated cardanol copolymer and MMA/cardanol/methoxylated cardanol terpolymer, and the evaluation of their photocrosslinking propensity, found to depend on the co-monomeric composition in accordance with the photosensitivity of the constituting cardanol-based monomers.

Experimental

Synthesis procedures

General comments and chemicals

Imidazole, tert-butyldimethylsilyl chloride, AD-mix α , tert-butanol, methanesulfonamide, sodium sulfite Na₂SO₃, sodium hydride NaH, iodomethane MeI, tetrabutyl ammonium fluoride TBAF, 2-bromoethanol, potassium carbonate K₂CO₃, triethylamine, acryloyl chloride, methyl methacrylate MMA, copper(I) bromide CuBr, ethyl α -bromoisobutyrate, ammonium chloride NH₄Cl and aluminium oxide Al₂O₃ neutral were purchased from Sigma-Aldrich (St Louis, MO). 4-dimethylaminopyridine DMAP, (N, N, N', N'', N''')-pentamethyldiethylenetriamine PMDETA and anisole were from Fluka (Seelze, Germany). Cardanol was bought from Cardolite (Mariakerke, Belgium). Dichloromethane CH₂Cl₂ and tetrahydrofuran THF (synthesis grade) were from Chem-Lab Analytical (Zedelgem, Belgium). CH₂Cl₂, n-heptane and ethyl acetate EtOAc for extraction and purification by column chromatography were from Fisher Scientific (Loughborough, UK). All reagents were used as received without preliminary purification. Compound numbers refer to Schemes 1 & 2. For the syntheses of **5**, **6** & **8** and following the last step described in their respective procedures, reactions were quenched by adding 250 mL of a saturated aqueous solution of NH₄Cl and the organic layer was extracted with EtOAc. For compounds **1-12**, the organic layers were washed with brine, dried over MgSO₄, filtered and finally concentrated under reduced pressure. In addition, intermediary products **1** and **3-5** were purified over silica gel (silica gel 60, 0.06-0.2 μ m) using heptane/CH₂Cl₂ (9/1 to 8/2), heptane/EtAc (9/1 to 0/10 and 2/8 to 0/10) and heptane/CH₂Cl₂ (9/1 to 8/2) respectively.

Cardoxy-tert-butyldimethylsilane (1)

Cardanol (10.0 g, 33.5 mmol), DMAP (409 mg, 3.40 mmol) and imidazole (3.65 g, 53.6 mmol) were dissolved in CH₂Cl₂ (100 mL). The solution was cooled to 0°C. Tert-butyldimethylsilyl chloride (6.06 g, 40.2 mmol) was added and the solution allowed to warm to room temperature while stirred overnight. The solution was filtered and evaporated under reduced pressure. The resulting oil was dissolved in Et₂O, washed with a saturated aqueous solution of NH₄Cl, the so-formed aqueous layer washed with Et₂O and the organic phases combined.

Hydroxylated carboxy-tert-butyldimethylsilane (2)

A mixture of AD-mix α (38 g) in tert-butanol/H₂O (1/1, 250 mL) was stirred until both phases became clear. Methanesulfonamide (1.4 g, 14.5 mmol) was added and the mixture was cooled to 0°C. A solution of **1** (6 g, 14.5 mmol) in tert-butanol/H₂O (1/1, 50 mL) was added and the reaction mixture was stirred vigorously at 0°C overnight. Na₂SO₃ (38 g) was added and the mixture was stirred for 30 min. The mixture was diluted with EtOAc and H₂O. The organic phase was washed with 20% aqueous NaOH solution.

Methoxylated carboxy-tert-butyldimethylsilane (3)

NaH (3.4 g, 0.14 mol) was added under stirring to a solution of **2** (8 g, 15.5 mmol) in THF (250 mL) at 0°C, followed by MeI (17.5 mL, 0.3 mol) after 5 min. After 10 min, the cooling bath was removed and the reaction mixture stirred to room temperature overnight. 200 mL of saturated aqueous NaCl solution were added and the organic layer was extracted with EtOAc.

Methoxylated cardanol (4)

TBAF (28.8 g, 110 mmol) in THF (110 mL) and **3** (6.5 g, 10.9 mmol) were stirred overnight at room temperature. After removal of THF, the residue was diluted with water and extracted with EtOAc. ¹H NMR (400MHz, CDCl₃): δ 7.12-6.64 (m/m, 4H, H_{Ar}), 3.47-3.16 (m, th:17.0H, exp:16.8H, CH₃-O, CH-OCH₃, CH₂-OCH₃), 2.55 (t, th:2.0, exp:2.1H, CH₂-Ar), 1.60-0.86 (m/m, th:20.5H, exp:20.6H, (CH₂)_n / CH₃) (Fig. 4c). Theoretical integrations (th) were calculated by considering the number of protons from the four components of cardanol convoluted by their natural occurrence^{13,14}. Measured integrations (exp) were evaluated by considering the four aromatic protons from the cardanol moiety as reference. Deviations to the theoretical values can occur owing to the purification steps.

2-bromoethoxy-tert-butyldimethylsilane (5) and carboxyethoxy-tert-butyldimethylsilane (6)

For the intermediary product **5**, 2-Bromoethanol (3.4 mL, 48 mmol) was dissolved in THF (240 mL) and placed in a 500 mL three-neck flask. Imidazole (4.2 g, 62 mmol) and tert-butyldimethylsilyl chloride (9.4 g, 62 mmol) were added under stirring and let to react for 5 h at room temperature. For the product **6**, cardanol (6 g, 20 mmol) was diluted in acetone (250 mL). **5** (14.4 g, 60 mmol) and K₂CO₃ (25 g, 20 mmol) were added and the mixture let to react under reflux for 44 h.

Cardoxyethanol (7) and Carboxyethanol acrylate CEAcry (8)

The procedure proposed for **4** has been similarly used for **7**, using TBAF (20.9 g, 80 mmol) in THF (80 mL) and **6** (3.7 g, 8.0 mmol). For the synthesis of **8**, triethylamine (0.85 mL, 6.1 mmol) was added to a solution of **7** (0.7 g, 2 mmol) in CH₂Cl₂ (50 mL), further cooled down to 0°C. Acryloyl chloride (0.55 mL, 6.1 mmol) diluted in CH₂Cl₂ (5 mL) was then added drop wise under vigorous stirring and the mixture stirred overnight under argon to warm to room temperature.

Hydroxylated carboxyethoxy-tert-butyldimethylsilane (9), Methoxylated carboxyethoxy-tert-butyldimethylsilane (10),

methoxylated carboxyethanol (11) and methoxylated carboxyethanol acrylate MCEAcry (12)

The procedure proposed for **2** has been similarly used for **9**, using AD-mix α (28 g) in tert-butanol/H₂O 1/1 (200 mL), methanesulfonamide (1 g, 10 mmol), **6** (4.5 g, 10 mmol) in t-butanol/H₂O 1/1 (50 mL) and Na₂SO₃ (28 g). The procedure proposed for **3** has been similarly used for **10**, using NaH (1.6 g, 0.066 mol), **9** (4.1 g, 7.3 mmol) in THF (125 mL) and MeI (8.2 mL, 0.132 mol). The procedure proposed for **7** has been similarly used for **11**, using TBAF (14.1 g, 54 mmol) in THF (54 mL) and **10** (3.5 g, 5.4 mmol). The procedure proposed for **8** has been similarly used for **12**, using triethylamine (0.8 mL, 5.7 mmol), **11** (1 g, 2 mmol) in CH₂Cl₂ (50 mL) and acryloyl chloride (0.5 mL, 5.7 mmol).

Poly(MMA-r-CEAcry) copolymer (13)

A first Schlenk flask was poured with MMA (0.83 g, 8.3 mmol), **8** (0.39 g, 1 mmol), PMDETA (31 μ L, 0.15 mmol) and anisole (6 mL). The liquid mixture was bubbled with argon for 60 min to remove oxygen, further transferred into a second Schlenk flask containing CuBr (11 mg, 0.1 mmol) and flushed with argon. Heated at 120°C and after 10 min stirring, ethyl α -bromoisobutyrate (13 μ L, 0.1 mmol) was added and the solution stirred overnight at 120°C. The polymerization was stopped by adding THF (10 ml) into the reaction mixture and air exposure. The mixture was passed through an Al₂O₃ column to remove residual copper species and the polymer finally precipitated in pentane. ¹H NMR (400MHz, CDCl₃): δ 7.18-6.74 (m/m, H_{Ar}), 5.82-5.01 (m/m/m, H_{vinyl} CH=CH₂ / CH= / CH₂=CH), 4.35-3.54 (m, CH₂O), 3.62 (m, CH₃-O-C(O)-), 2.80 (m, CH=CH-CH₂-CH=CH), 2.57 (m, CH₂-Ar), 2.06-0.84 (m, CH₂-CH=, CH₂-CH₂-Ar, (CH₂)_n, CH₃) (Fig. 7a).

Poly(MMA-r-MCEAcry) copolymer (14)

The procedure proposed for **13** has been similarly used for **14**, using MMA (0.5 g, 5 mmol), **12** (0.35 g, 0.6 mmol), PMDETA (19 μ L, 0.09 mmol), anisole (4 mL), CuBr (6.5 mg, 0.04 mmol) and ethyl α -bromoisobutyrate (8 μ L, 0.1 mmol). ¹H NMR (400MHz, CDCl₃): δ 7.18 (m, H_{Ar}), 6.74 (m, H_{Ar}), 4.35 (m, CH₂O), 3.62 (m, CH₃-O-C(O)-), 3.43 (m, CH₃O), 2.56 (m, CH₂-Ar), 2.19-0.84 (m, CH₂-CH₂-Ar, (CH₂)_n, CH₃) (Fig. 7b).

Poly(MMA-r-CEAcry-r-MCEAcry) terpolymer (15)

The procedure proposed for **13** has been similarly used for **15**, using MMA (1.8 g, 18 mmol), **8** (430 mg, 1.1 mmol), **12** (640 mg, 1.1 mmol), PMDETA (75 μ L, 0.36 mmol), anisole (10 mL), CuBr (27 mg, 0.2 mmol) and ethyl α -bromoisobutyrate (33 μ L, 0.2 mmol). ¹H NMR (400MHz, CDCl₃): δ 7.18 (m, H_{Ar}, 1H), 6.74 (m, H_{Ar}, 3H), 5.38 (m, CH=, th), 4.34 (m, CH₂O), 3.62 (m, CH₃-O-C(O)-), 3.43 (m, CH₃O), 2.57 (m, CH₂-Ar), 2.06-0.84 (m, CH₂-CH=, CH₂-CH₂-Ar, (CH₂)_n, CH₃) (Fig. 7c).

Photoaging and photopolymerization

Samples were exposed to UV-visible irradiation by means of a Suntest CPS+ system (Rycobel, Deerlijk, Belgium) at 35°C in

presence of oxygen.¹⁰ The device is equipped with a xenon lamp for irradiation at wavelengths longer than 290 nm. A black panel controls the irradiance at 400 W/m². For cardanol and methoxylated cardanol, 50 μ L of pure chemical have been deposited on a glass slide (~ 20 mm x 20 mm), gently rotated at 500 rpm to form a homogeneous film further submitted to photopolymerization. The thickness has been evaluated by means of a Nanoscratch tester from CSM Instruments (Peseux, Switzerland) at 100 μ m for cardanol after 96 h of UV exposure. For polymers, 500 μ L of a polymer solution in THF (20 mg mL⁻¹) have been deposited on a glass slide (20 mm x 20 mm) and allowed to air dry. The thickness measured by nanoscratch has been found around 6 μ m for each sample. Aiming at providing results about the chemical and molecular changes undergone by cardanol and derivatives under UV activation by implementing a complete analytical strategy, kinetics of photocrosslinking and thicknesses considerations are out of the scope of the following discussion. Consequently, exposure times are indicative and a unique UV-exposed sample will be presented in each section, considered as sufficiently representative of the underlying processes behind the UV exposure.

Characterizations

SEC, SEC-MS and SEC-UV/Vis off-line couplings

The SEC apparatus consisted of a 600E controller & pumping units (Waters, Versailles, France) followed by a 486 Tunable UV/Vis detector (Waters). Separation was performed on a unique mixed bed column (PLgel Mixed-D 300x7.5 mm, particle size 5 μ m, Agilent) with precolumn (PLgel Mixed-D 50x7.5 mm) at room temperature. THF was used as eluent at a flow rate of 1 mL min⁻¹, while 20 microliters of a 15 g L⁻¹ resin solution was injected to record satisfactory SEC-MS and SEC-UV/Vis spectra in a single run. Polystyrene standards of molecular weights MW 35,000, 3,700 and 2,000 g mol⁻¹ (Sigma Aldrich) were used as calibrants to estimate the MW of the samples. In SEC-MS coupling, collected fractions were allowed to evaporate for a couple of minutes and the residual solution submitted to mass analysis. In SEC-UV/Vis coupling, collected fractions were directly submitted to a UV/Vis analysis with THF used in the SEC elution as blank.

Mass spectrometry

Mass spectra were recorded using a Autoflex III mass spectrometer (Bruker, Leipzig, Germany) equipped with a frequency-tripled Nd-YAG laser (λ =355 nm) operating at a pulse rate of 50 Hz. The time-of-flight analyzer was operated in reflectron mode. External calibrations were performed using monodisperse poly(ethylene glycol) PEG (Sigma-Aldrich, 600, 1,500 and 4,000 g mol⁻¹) in the positive ion mode and clusters of an orange azoic pigment (C₃₂H₂₄N₈O₂Cl₂, CAS: 3520-72-7) in the negative ion mode. FlexControl software version 3.0 (Bruker) was used for instrument control and data acquisition, while both FlexAnalysis software version 3.0 (Bruker) and mMass version 5.5¹⁵ were used for data processing. In matrix assisted laser desorption ionization mass spectrometry in the

positive ion mode (MALDI(+)-MS), samples were mixed with grains of matrix (trans-2-[3-(4-tert-Butylphenyl)-2-methyl-2-propenylidene]malononitrile DCTB, Sigma-Aldrich) and salt (LiTFA or AgTFA, Sigma-Aldrich), gently ground using mortar/pestle, the resulting powder further deposited onto the target and pressed gently with a small spatula to produce a homogeneous thin coverage (solvent-free sample preparation^{16,17}). In surface assisted laser desorption ionization mass spectrometry in the negative mode (SALDI(-)-MS), samples were dissolved in THF and mixed with a suspension of carbon nanofibers GANF (Grupo Antolin, Spain) in acetone, the mixture deposited on the target and allowed to air dry before the mass analysis.

UV/Vis, FTIR and nuclear magnetic resonance spectroscopies

UV/Vis spectra were recorded using a Lambda 35 UV/Vis spectrometer (PerkinElmer, Waltham, MA) with 500 μL quartz cuvettes and THF HPLC grade used as eluent for the isocratic SEC analyses (*vide supra*). FTIR spectra were recorded using a Tensor 27 spectrometer (Bruker Optics, Bruxelles, Belgium) in transmission mode on KBr pellet. The spectra were obtained from 32 scans at a resolution of 4 cm^{-1} between 4000 to 600 cm^{-1} . The ^1H nuclear magnetic resonance (NMR) characterization was performed on a Avance 400 spectrometer (Bruker Biospin, Wissembourg, France) equipped with a 9.4 T Ascend magnet, operating at a proton frequency of 400 MHz. Samples were dissolved in CDCl_3 with all peaks referenced relative to tetramethylsilane.

Results and discussion

Highlighting the photosensitivity of cardanol by FTIR and SEC

Despite its expected propensity for photopolymerization owing to its structural feature, and to the best of our knowledge, the behavior of cardanol under UV exposure has not been reported in the literature. Pristine cardanol has been deposited as a thick film on a glass substrate (evaluated at a hundred microns at the end of a 96 h irradiation). After 48h of exposure to UV irradiation, the light yellow liquid of low viscosity turned into a 50% insoluble highly viscous liquid and a 85% insoluble wax was obtained after 96 h, exhibiting a dark yellow color (ESI†), confirming that cardanol is highly photosensitive and undoubtedly undergoes crosslinking. Its UV/Vis absorption spectrum is also found to noticeably change, with a shouldering of the absorbance towards longer wavelengths (ESI†) from which the yellowing phenomenon is originating. FTIR spectra of pristine and 96 h UV-exposed cardanol are depicted in Fig. 1a&b, the former being superimposed in light grey line on Fig. 1b for sake of easier comparison. Among other changes, the appearance of a carbonyl band at 1722 cm^{-1} is typical of polymer photoproducts under (accelerated) ageing through light exposure. The decrease – rather than disappearance – of bands at 3011 cm^{-1} , 1590 cm^{-1} and 748 cm^{-1} ($\text{C}=\text{C}$ from alkenes)^{18,19} denotes a substantial consumption of the unsaturations borne by the cardanol side chain.

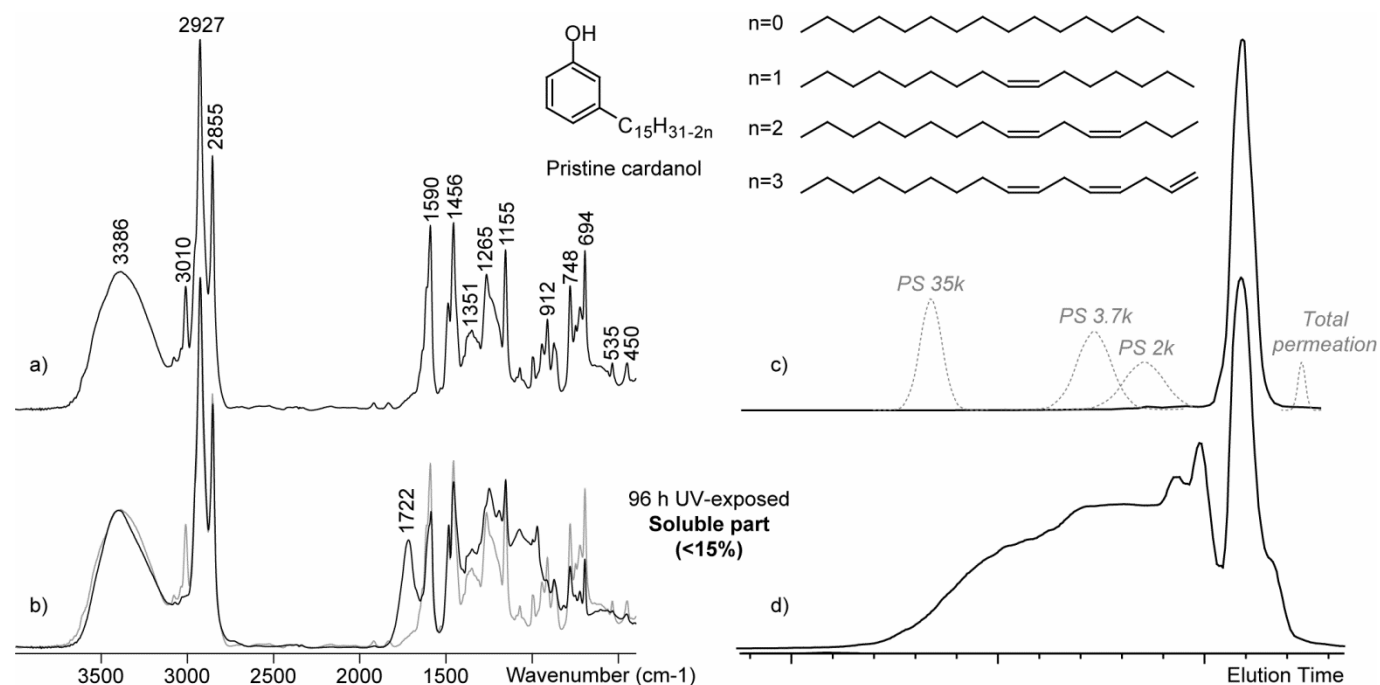


Fig. 1. FTIR spectra of a) pristine and b) 96 h UV-exposed cardanol. FTIR spectrum of pristine cardanol is also superimposed on b) (light grey line). SEC chromatograms of c) pristine and d) 96 h UV-exposed cardanol. SEC chromatogram of PS standards (35,000, 3,700 and 2,000 g mol^{-1}) is superimposed on c) to estimate the MW.

Cardanol and even more its associated UV-exposed counterpart are formed of several components. The increase of viscosity and the decrease of solubility undoubtedly reveal underlying

polymerization and cross-linking processes. With such a complex sample, additional analytical techniques should be proposed to comprehend these polymerization processes, beyond

the chemical insights provided by FTIR. SEC appears as a well-suited analytical tool to highlight any changes in the MW, themselves pointing out the polymerization processes. The SEC chromatograms of pristine cardanol and the soluble part (~15%) of the 96 h UV-exposed cardanol are depicted in Fig. 1c&d respectively, recorded with a UV detector set at 280 nm⁹ (a local UV absorption maximum of pristine cardanol, ESI†). As compared to the chromatogram of pristine cardanol exhibiting a unique fine “monomer” peak, the occurrence of high MW materials after UV exposure is readily found with a strong signal towards the shortest elution times. Contributions from “dimers” and “trimers” are clearly separated from the “monomer” peak while the largest oligomers constitute a shouldering with no resolution. Those arbitrary assignments will be further validated by a SEC-MALDI(+)-MS coupling. Such polymerization process found in the (limited) soluble part of the photopolymerized sample should be extrapolated into crosslinking processes to account for the main insoluble part. With PB as a reference, these processes probably occur through the abstraction of the reactive hydrogen(s) in alpha position of the unsaturations borne by the C15 side chain, forming radical species prone to enter into polymerization through C-O-C or C-C linkages with other unsaturated congeners.^{10,20} Similar observations have been reported for the photoaging of vegetable oils.²¹ As a short digression and still following the PB reference behavior, a small shouldering towards the longer elution times compared to the “monomer” peak is also observed, pointing out some cleavage processes accompanying the polymerization route leading to short structures bearing either the phenol moiety or a part of the side chain (not seen with a UV detector).¹⁰ Superimposed on Fig. 1c is the SEC chromatogram of the co-elution of three PS standards (MW 35,000, 3,700 and 2,000 g mol⁻¹) and detected in that order of elution (grey line, recorded at $\lambda=254$ nm). MW of the soluble photoproducts from the 96 h UV-exposed cardanol thus ranges from a few hundred g mol⁻¹ (smallest photo products near the total permeation peak) to more than 30,000 g mol⁻¹ PS equivalent. These largest products correspond to the coupling of around ten cardanol moieties. To better understand the polymerization processes behind this increase of MW, mass spectrometry has been used and the results reported in the following section. Mass spectrometry has indeed been recently proposed as a powerful tool for the analysis of cardanol and cardanol derivatives.^{22,23} In particular, MALDI(+)-MS²⁴ and its emphasis on the so-called “unsaturation pattern” arising from the tri-, di-, mono-unsaturated and saturated components composing cardanol has allowed thorough insights into the chemistry of cardanol to be gained.²⁵

Mass spectrometry and off-line SEC-MS coupling: the implication of the side chain in cardanol photosensitivity

A rapid mass analysis of the pristine and 96 h UV-exposed cardanol samples focused on the unsaturation pattern gives rise to the restricted MALDI(+)-MS spectra depicted in Fig. 2. The four peaks spaced by 2 Da are assigned to the three main tri-, di- and mono-unsaturated compounds convoluted by a silver cation (the saturated component is of too low relative abundance to be

visualized owing to the isotope contributions). A strong distortion of the unsaturation pattern is observed between the pristine (Fig. 2a) and the UV-exposed (soluble) sample (Fig. 2b). Simulation of the unsaturation patterns²⁵ allows the composition of tri-/di-/mono-unsaturated species to be evaluated (insets in Fig. 2). Considering the tri-unsaturated congener at m/z 405/407 (tri-unsaturated cardanol + ¹⁰⁷Ag/¹⁰⁹Ag), a drastic reduction from 41% to 10% of its abundance is readily observed, in accordance with the preliminary FTIR data. Those highly unsaturated species are indeed more prone to a) lose a H radical in alpha position and be oxidized and b) react with the so-formed alkoxyde or alkyl radicals. The more the number of unsaturations, the higher the probability to react with radicals. Mass spectrometry is a unique analytical tool to explore the molecular composition of samples. MALDI-MS is nevertheless notoriously biased by the dispersity of polymers,²⁶ owing to desorption, ionization and detection efficiencies issues (in case of a secondary electron detector), all favorable to the lowest molecular weight species. In polydisperse samples for which “small” and “large” species coexist, only the smallest structures would be over-detected while the largest will not be observed at all.

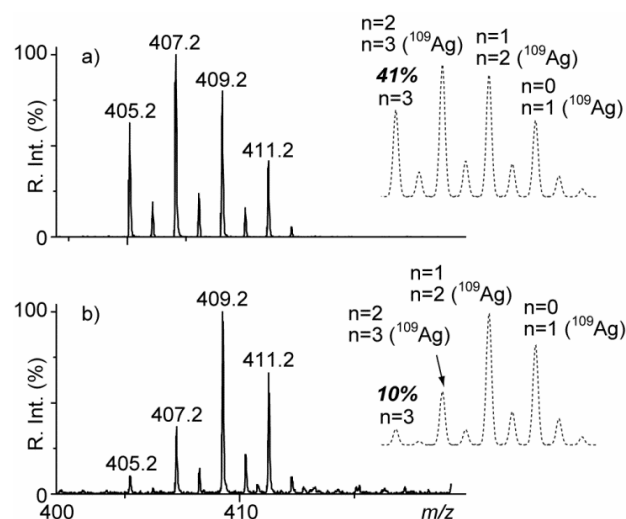


Fig. 2. Restricted MALDI mass spectra of a) pristine and b) 96h UV-exposed cardanol focused on the silverated cardanol. Simulated unsaturation patterns are depicted in insets with peaks assignment and the relative abundance of tri-unsaturated component.

The SEC chromatogram of the 96 h UV-exposed sample (Fig. 1d) exhibits the fingerprint of a highly polydisperse material, leading to biased direct MALDI(+)-MS spectra unable to display the oligomeric species (data not shown). To overcome this inherent discrimination, an off/on-line coupling of SEC and mass spectrometry constitutes an elegant and easy-to-handle analytical strategy.²⁷⁻²⁹ Fractionating a polydisperse sample by the way of SEC separation (*i.e.* based on the gyration radius in solution, further correlated to the molecular weight) into several aliquots allows those so-collected “monodisperse” fractions to be mass-analyzed independently with a drastically limited bias. From the SEC elution of the 96 h UV-exposed sample, three fractions have

been collected and thought to consist in “monomers”, “dimers” and “trimers” of cardanol. The collected fractions have been re-analyzed by SEC to check at their purity (ESI[†]) and further mass-analyzed by MALDI(+)-MS (Fig. 3a-c respectively). Owing to a poor signal-to-noise ratio, m/z ranges of the MALDI(+)-MS spectra have been restricted around the peaks of interest, but it is worth mentioning no other cardanol-based species were found in the whole mass spectra. In the MALDI(+)-MS spectrum of the “monomer” fraction (Fig. 3a), in addition to the silverated cardanol at m/z 409 (+ congeners) are detected two oxidized species adducted with Ag⁺ at m/z 425 + congeners (+16 Da = + O/OH) and at m/z 439 + congeners (+32Da = +2*O/OH). Structures of these two new species could be figured out by considering a cardanol moiety with one or two hydrogen atoms in alpha position of the unsaturations replaced by one or two O/OH groups. These oxidized products have been already proposed as photo-products of PB¹⁰ and vegetable oils.²¹ In the

“dimer” mass spectrum (Fig. 3b), two species are readily detected at m/z 723 (+ congeners) and m/z 739 (+ congeners). Their elemental compositions are those of two cardanol moieties plus one or two O/OH groups, respectively. Structurally speaking, a dimer of cardanol with a) an oxo bridge between the two side chains and b) an oxo bridge and an additional O/OH group along one of the two side chains constitute satisfactory representations of these two species. By the way, the production of such dimers has involved a double bond of one cardanol moiety and their detection corroborates the consumption of the more unsaturated cardanol components highlighted by FTIR and MALDI(+)-MS (Fig. 1&2). The “trimer” mass spectrum (Fig. 3c) finally displays three species detected at m/z 1021 (+ congeners), m/z 1037 (+ congeners) and m/z 1053 (+ congeners), readily seen as trimers of cardanol whose side chains are linked by one O atom, plus one or two O/OH groups along the side chains, respectively.

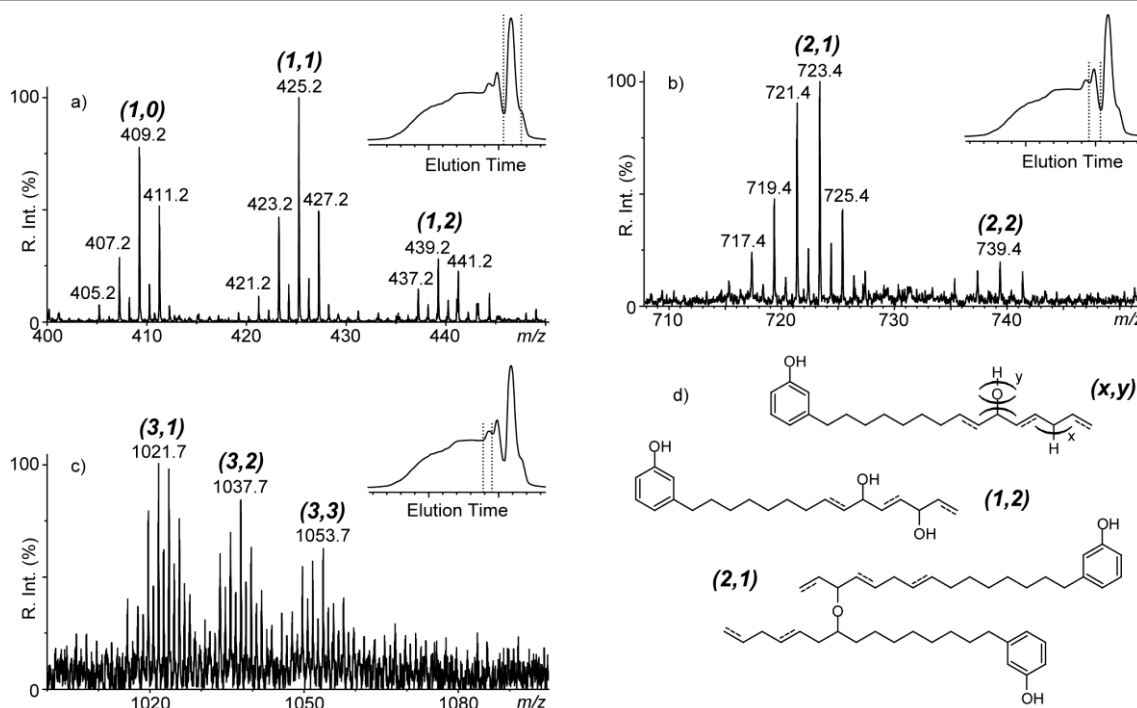


Fig. 3. SEC-MALDI(+)-MS mass spectra of fractions collected from the SEC elution of a 96 h UV-exposed cardanol. a) m/z 400 – m/z 450 (monomers peak), b) m/z 710 – m/z 750 (dimers peak), c) m/z 1000 – m/z 1100 (trimers peak). Species are named using the nomenclature scheme (x,y) described in d) where x designates the number of cardanol moieties and y the number of supernumerary oxygen atoms. SEC chromatograms with the fraction of interest are depicted in insets.

Incidentally, the UV/Vis spectra of the so-collected fractions have also been recorded to better estimate the contribution of each fraction (“monomer”, “dimer”, trimer” and “oligomer”) to the change in the UV/Vis spectrum of the UV-exposed sample (ESI[†]). The UV/vis spectrum of the “monomer” fraction remains highly similar to the UV/Vis spectrum of pristine cardanol with a double maximum at $\lambda=273$ / 280 nm and a huge decrease of the absorbance beyond 300 nm (relative absorbance at 300 nm: 0.05). The UV/Vis spectrum of the dimeric fraction exhibits a noticeable shouldering towards longer wavelengths (relative abundances at 300 nm: 0.1) while the double maximum tends to merge into a single peak at $\lambda=273$ nm. UV/Vis spectra of

“trimer” and “oligomer” fractions follow the same trend, displaying an even more pronounced shouldering towards visible wavelengths (relative abundances at 300 nm: 0.15 and 0.20, respectively). Accompanying the polymerization/cross-linking processes highlighted by the SEC chromatograms is also a strong yellowing of the material (from a light yellow to a dark orange color). From these SEC-UV/Vis spectra, it seems reasonable to conclude the dimers/trimers/oligomers account for this yellowing. The rather limited shouldering of their UV/Vis spectra is in accordance with C-O-C or C-C linkages between the C15 side chains (remote from the phenolic chromophore). However, possible coupling involving the phenol groups³⁰

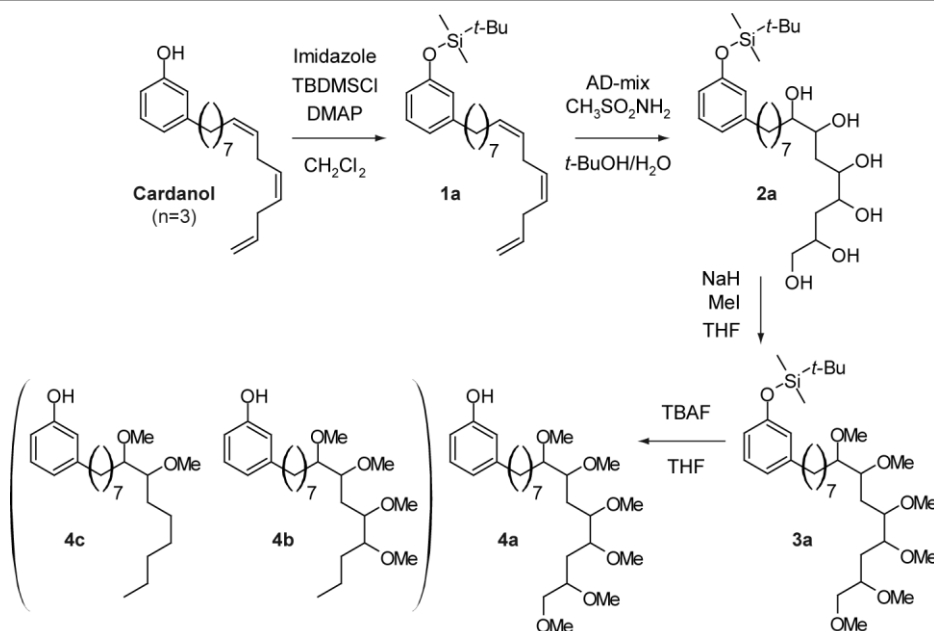
cannot be dismissed and would also lead to the production of polycardanol species, accounting for the noticeable modification of the double peak maximum at 273 and 280 nm merging into a single absorbance maximum. It is obvious several isomeric products constitute a given species detected in the SEC-MALDI(+)-MS and SEC-UV/Vis spectra owing to the number of unsaturations borne by the C15 side chains. For sake of clarity and following our proposal for the characterization of cardanol derivatives,²⁵ a simple nomenclature is proposed in Fig. 3d to simply name the products formed upon UV exposure. This nomenclature would moreover be more accurate than a unique structure which would make other isomers implicitly not considered. A (x,y) denomination appears sufficiently precise, with x the number of cardanol moieties ($C_{15}H_{31-2n}C_6H_3OH$) and y the number of supernumerary oxygen atoms (either O or OH, linking the cardanol side chains or as hydroxy pendant groups) as compared to a pristine cardanol chemical composition. Two examples of structures found in the SEC-MALDI(+)-MS spectra are depicted in Fig. 3d and named with their (x,y) nomenclature: a cardanol moiety bearing two hydroxy groups in lieu of the hydrogen atoms in alpha positions named (1,2) and two cardanol moieties linked by an oxygen atom named (2,1). Despite several structures could be drawn for each (x,y) couple, this nomenclature allows the patterns found in a mass spectrum to be identified unequivocally. The monomeric, dimeric and trimeric photo-products found in the SEC-MALDI(+)-MS spectra of the 96 h UV-exposed cardanol have been subsequently named using this simple nomenclature (Fig. 3a-c). Interestingly, the (3,1) trimeric species found in Fig. 3c should contain either a C-C linkage between side chains¹⁰ and/or a phenol/phenol coupling (cf. the SEC-UV/Vis spectra, ESI⁺), in both cases with no additional oxygen atom as oxo bridge.

A side chain functionalization to reduce the photosensitivity

As profusely demonstrated above, cardanol is highly photosensitive, with a high propensity of its C15 polyunsaturated side chain to enter into polymerization and cross-linking until a *fully insoluble* material is produced. In order to reduce the UV sensitivity of cardanol, the functionalization of its side chain to replace unsaturations by other functional groups appears as a promising route. Several procedures have already been described in the literature.^{6,7} If the use of the saturated component only (n=0, pentadecyl phenol, also known as hydrogenated cardanol HC³¹) would also limit the photosensitivity, its poor natural occurrence would make its extraction tedious and extremely time-consuming by preparative chromatography.³² In addition, its preparation by hydrogenation of cardanol over palladium catalyst³³ would require expensive synthesis equipment. On the contrary and despite a multi-step route, modifying the side chain remains a cheap procedure and allows a consequent number of functional groups to be added, further improving the compatibility of cardanol with other chemicals or polymers in a composite system and authorizing unlimited applications.

Synthesis and characterization of methoxylated cardanol

Methoxylation of the side chain has been specifically chosen in order to turn cardanol into a UV resistant derivative, the methoxy groups being expected to remain inert towards UV irradiation in the timeframe pristine cardanol would have turned into an insoluble wax. The synthesis procedure used for the functionalization of the C15 side chain with methoxy groups in lieu of the C=C unsaturations is summed up in Scheme 1 with the detail of all the steps exemplified for the tri-unsaturated congener (n=3).



Scheme 1. Synthesis route for the methoxylation of cardanol. For sake of clarity, in the main route is represented the tri-unsaturated congener (n=3) only with the associated hydroxylated (**2a**) and methoxylated derivatives (**3a** & **4a**). The other targeted structures from di- (n=2) and mono-unsaturated (n=1) congeners are given in brackets (**4b** & **4c**, resp.).

Starting from pristine cardanol, the phenol moiety was first protected with a silylated group using tert-butyldimethylsilyl chloride to yield the so-called carboxy-tert-butyldimethylsilyl 1 (ESI[†] for MALDI(+)-MS spectra along with additional comments). In the literature, the hydroxylation of the unsaturated side chain of cardanol is performed in two steps: 1) double bonds are first epoxidized and 2) polyols are obtained under acidic hydrolysis.³⁴ Here is proposed a one-step dihydroxylation using AD-mix α ³⁵ as catalyst. The hydroxylated carboxy-tert-butyldimethylsilyl 2 was produced with a quantitative yield (ESI[†] for MALDI(+)-MS spectra). The methylation of the hydroxyl groups was performed using iodomethane and sodium hydride to yield the methoxylated carboxy-tert-butyldimethylsilyl 3 (ESI[†] for MALDI(+)-MS spectra). The deprotection of the phenol group was finally conducted using a 1M tetrabutyl ammonium fluoride solution. The targeted methoxylated cardanol 4 was isolated and further submitted to FTIR, MS and NMR analyses before its exposure to UV irradiation and the subsequent analysis of the photo-products. Characterizations of the so-synthesized methoxylated cardanol are compiled in Fig. 4. As compared to the pristine cardanol, the occurrence of two strong bands at 2828 and 1109 cm⁻¹ in the FTIR spectrum of 4 is in accordance with the expected methoxylation (Fig. 4a). To avoid the deleterious adduction of DCTB²⁵ unexpectedly faced with this new cardanol derivative (ESI[†]) and since the phenol group has been left intact with its slightly acidic hydrogen, a mass analysis in the *negative* ion mode has been conducted and shown to provide satisfactory mass spectra. The SALDI(-)-MS spectrum of 4 is depicted in Fig. 4b. The targeted methoxylated constituents of cardanol are readily seen at *m/z* 363 (deprotonated 4c, *n*=1), *m/z* 423 (deprotonated 4b, *n*=2) and *m/z* 483 (deprotonated 4a, *n*=3). Interestingly, the fully saturated congener is also slightly observed at *m/z* 303, bearing no methoxy groups along its side chain. It is finally worth mentioning hydroxylation and subsequent methoxylation of the C15 side chain leads to a *degeneracy* of the unsaturation pattern. While forming a narrow pattern with peaks spaced by +/- 2 Da in the mass spectrum of pristine cardanol (Fig. 4b, light grey line), with *m/z* *n*=3 < *m/z* *n*=2 < *m/z* *n*=1, hydroxylated and methoxylated cardanol exhibit instead three *distinct* peaks spaced by 32 Da and 60 Da, with an inversion of the *m/z* order: *m/z* *n*=1 (two OH or OMe) < *m/z* *n*=2 (four OH or OMe) < *m/z* *n*=3 (six OH or OMe) (Fig 5b and ESI[†]). The ¹H NMR spectrum of the methoxylated cardanol is finally depicted in Fig. 4c. The pattern at 3.3 ppm is of particular interest since it is arising from the protons of the so-added methoxy groups and protons of the CH groups from the C15 side chain. As compared to the ¹H NMR spectrum of pristine cardanol⁸ depicted with light grey line in Fig. 4c, no more signal from the unsaturations along the side chain is found between 5.0 and 5.8 ppm, ensuring a quantitative yield. Residual tert-butyldimethylsilyl fluoride formed upon the deprotection of phenol is still found despite the purification step (two peaks at 0.9 and 0.1 ppm noted with asterisks). The tert-butyldimethylsilyl fluoride / methoxylated cardanol molar ratio does nevertheless not exceed 1:3 (considering the peak areas)

and owing to its inertness towards UV exposure, such impurity will not be further considered. For sake of clarity, the 4b congener (tetramethoxylated cardanol) is depicted in inset and the detected peaks assigned accordingly with letters. Theoretical integrations have been calculated by considering the proton amounts from the three components 4a-c convoluted by their relative abundance,^{13,14} while the measured integrations from the ¹H NMR spectrum have been evaluated considering the four aromatic protons (at 6.7 and 7.1 ppm) as the reference value.

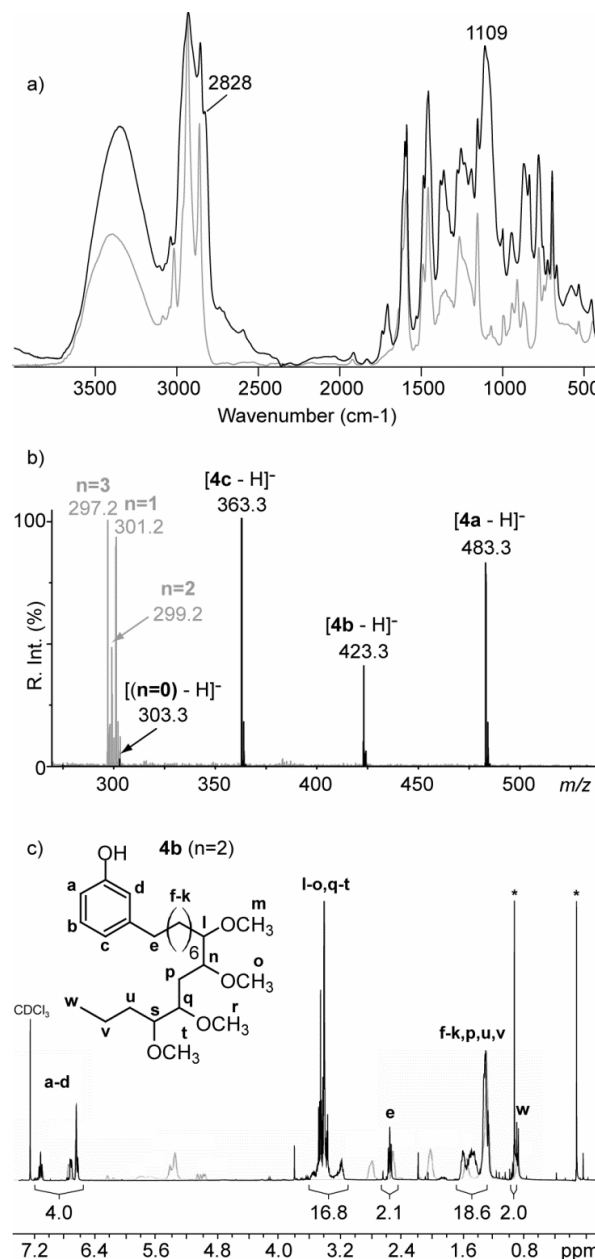


Fig. 4. a) FTIR spectrum, b) SALDI(-)-MS spectrum and c) ¹H-NMR spectrum of methoxylated cardanol 4. The 4b (*n*=2) congener is depicted in inset of c) and peaks assigned accordingly. The two other 4a (*n*=3) and 4c (*n*=1) congeners are nevertheless considered in the integrations. FTIR, SALDI(-)-MS and ¹H-NMR spectra of native cardanol are also superimposed on a-c) in light grey line.

UV exposure and characterization of the photo-products

Methoxylated cardanol thick films (~ 100 μm) remained *fully soluble* in THF even after 170 h of UV exposure (3.5 times longer than cardanol which turned into a 50% insoluble wax after 48 h of exposure), with a noticeable increase of its viscosity. However, if the cross-linking process has been considerably lowered no to say avoided by the methoxylation of the side chain, it did not prevent the yellowing of the sample (ESI†). Concomitantly, its UV/Vis spectrum also displays a prominent shouldering towards visible wavelength (ESI†). Echoing the characterizations done for cardanol, FTIR, SEC, SEC-SALDI(-)-MS and SEC-UV/Vis analyses have been conducted to better comprehend the ageing processes. The FTIR spectra of pristine and 170 h UV-exposed methoxylated cardanol **4** are depicted in Fig. 5a&b. Among the noticeable differences, one should notice a huge diminution of the –OH band at 3345 cm⁻¹ which strongly differ from the FTIR fingerprints of aged vs. pristine cardanol (Fig. 1b). Relative abundance of the bands from the methoxy groups are very slightly decreasing, while a typical band at 1729 cm⁻¹ associated with carbonyl photoproducts is appearing, indicating that methoxylated cardanol is rather resistant but not insensitive to UV irradiation. SEC analysis has been carried out

to better understand the origin of the increase of the viscosity, probably due to unexpected oligomerization processes. The SEC chromatograms of pristine and 170 h UV-exposed methoxylated cardanol are depicted in Fig. 5c&d. A strong propensity for *dimerization* is readily found in the SEC chromatogram of the photopolymerized methoxylated cardanol. The so-called “dimer” peak is indeed not exceeding 4,000 g mol⁻¹ PS equivalent (Fig. 5c). Its broadness could be accounted for by considering the six dimers potentially produced from the three monomers constituting the methoxylated cardanol (dimethoxylated, tetramethoxylated and hexamethoxylated) and their radius of gyration which probably largely differ. The clear discrimination between the hexamethoxylated cardanol (**4a**, *m*=3) and the two tetramethoxylated and dimethoxylated (**4b**&**c**, *m*=2 and *m*=1) in the “monomer” peak of pristine methoxylated cardanol (Fig. 5c) supports this assumption. The production of dimers *only* remains not clearly understood at the time of writing, but undoubtedly accounts for the full solubility of the UV-exposed sample in THF, and indirectly validates the oligomerization / cross-linking process through the double bonds for the *native* cardanol.

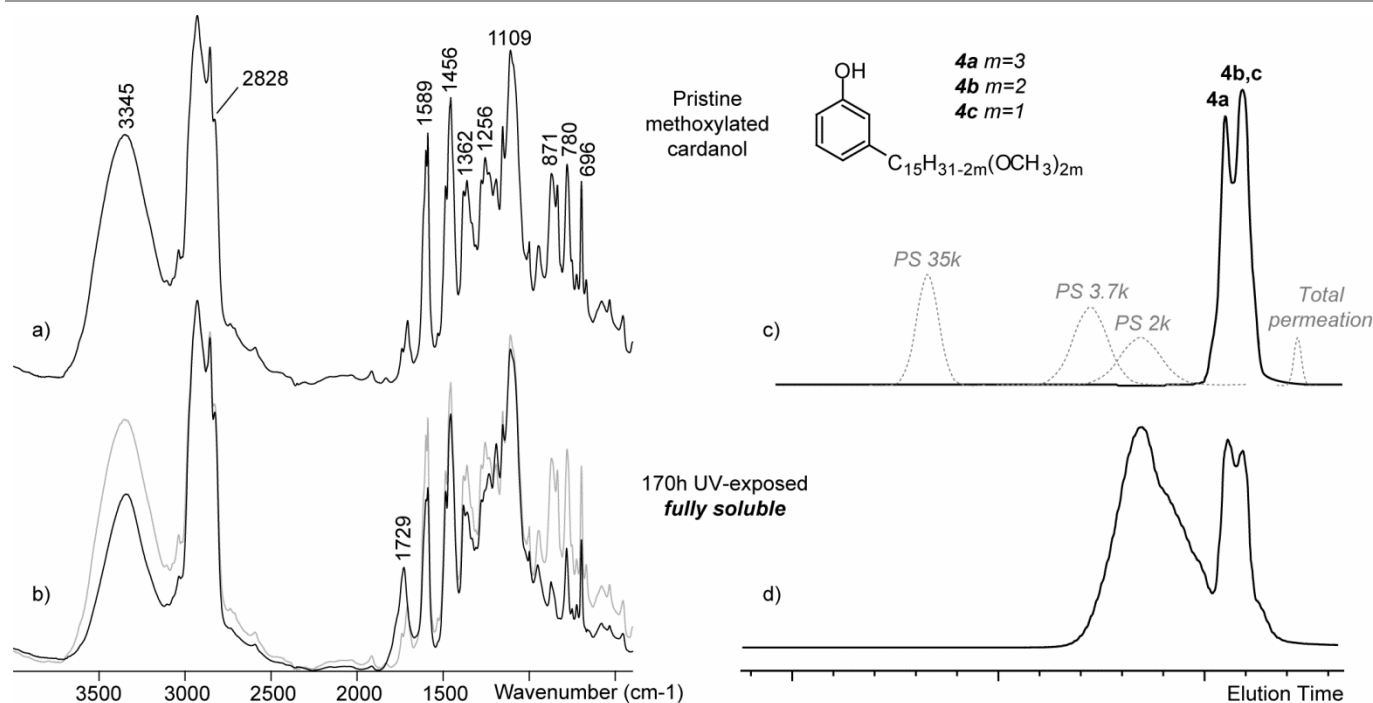


Fig. 5. FTIR spectra of a) pristine and b) 170 h UV-exposed methoxylated cardanol **4**. FTIR spectrum of pristine methoxylated cardanol is also superimposed in b) (light grey line) for sake of comparison. SEC chromatograms of a) pristine and b) 170 h UV-exposed **4**. Note the UV-exposed sample remains fully soluble. SEC chromatogram of PS standards (35,000, 3,700 and 2,000 g mol⁻¹) is superimposed on c) to estimate the MW.

Following the analytical methodology proposed for cardanol, “monomer” and “dimer” fractions from the SEC elution of the 170 h UV-exposed methoxylated cardanol have been subsequently mass analyzed in SALDI(-)-MS (Fig. 6a&b) and their associated UV/Vis spectra recorded separately and depicted in Fig. 6c&d. Collected fractions have been re-analyzed by SEC to ensure their purity (ESI†). The mass spectrum of the “monomer” peak (Fig. 6a) is highly similar to the SALDI(-)-MS

spectrum of pristine methoxylated cardanol **4** prior to any UV irradiation (Fig. 4b). However, the detection of ions of very limited relative abundances at *m/z* 379 (+16 Da from **4c**), *m/z* 439 (+16 Da from **4b**) and *m/z* 499 (+16 Da from **4a**) highlights the occurrence of oxidative processes during the irradiation. In addition, the production of hydroxy groups from methoxy groups through demethylation (as reported by Lachman et al for the thermal ageing of polyphenols³⁶) is shown by the detection of

species of lower molecular weights at m/z 349 (-14 Da from **4c**), m/z 409 (-14 Da from **4b**) and m/z 469 (-14 Da from **4a**). This could account for the slight decrease of the MeO bands in the FTIR spectrum of the UV-exposed methoxylated cardanol (Fig. 5b). The SALDI(-)-MS spectrum of the “dimer” fraction is depicted in Fig. 6b. Deprotonated dimers are readily observed with a varying number of methoxy groups (from 4 at m/z 725.6 to 12 at m/z 965.7). Based on their chemical composition and according to the nomenclature proposed in the previous section (Fig. 3d), those dimers should be noted (2,0) since they are formed of two (methoxylated) cardanol moieties but no additional (bridging) oxygen atoms. Considering that last point, and since no more unsaturation along the side chain could lead to carbon-carbon bonding, the dimerization process has been speculated to occur through a phenol group with a Ph-O-Ph ether linkage.³⁰ This structural consideration nicely accounts for the dramatic decrease of the -OH band observed in the FTIR spectrum of the UV-exposed methoxylated cardanol (Fig. 5b). The UV/vis spectrum of the “monomer” fraction (Fig. 6c)

remains similar to the UV/vis spectrum of pristine methoxylated cardanol (ESI†) with a double maximum at 273/280 nm and the absence of absorbance above 300 nm (relative absorbance at 300 nm: 0.04), thus indicating the photoproducts found in FTIR and SALDI(-)-MS do not constitute the main part of this “monomer” fraction. On the contrary, the UV/Vis spectrum of the “dimer” fraction depicted in Fig. 6d strongly deviate from the “monomer” fingerprint with the disappearance of the double maximum absorption at 273 and 280 nm – replaced by a unique maximum at 275 nm – and a highly pronounced shouldering towards higher wavelengths (relative absorbance at 300 nm: 0.42). Even dimers from the UV-exposed cardanol (ESI†) whose UV/Vis spectrum has been depicted with dashed line in Fig. 6d for sake of reminder and comparison do not exhibit such drastic change in their absorption property (relative absorbance at 300 nm: 0.10). This last experiment makes the Ph-O-Ph bridging – that is to say involving the phenolic chromophores – even more probable and meaningful, and indirectly validates the C15-O-C15 linkage proposed for cardanol.

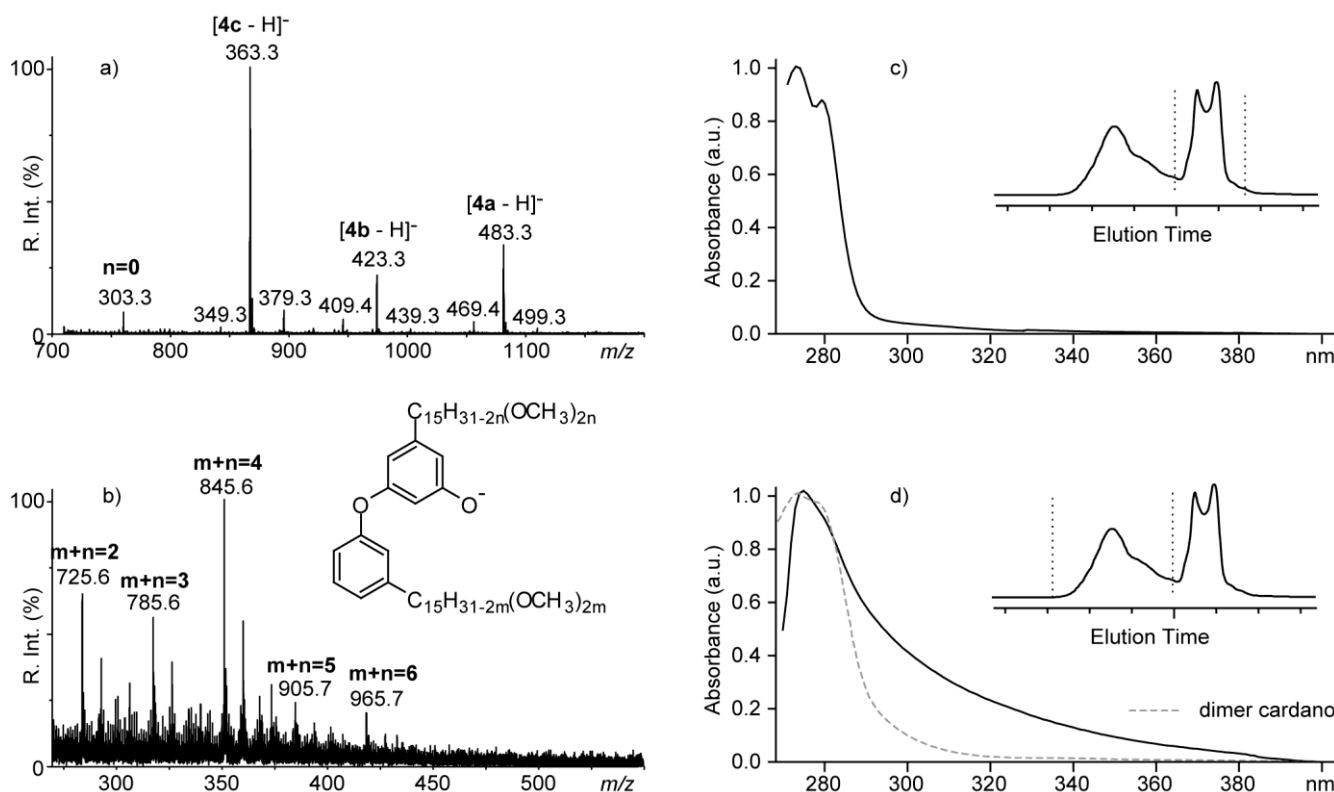


Fig. 6. SEC-SALDI(-)-MS mass spectra of fractions collected from the SEC elution of a 170 h UV-exposed methoxylated cardanol **4**. a) m/z 300 – m/z 550 (monomers peak), b) m/z 700 – m/z 1200 (dimers peak). c-d) UV/Vis spectra of the same fractions. SEC chromatograms with the fraction of interest are depicted in insets.

Functionalization of the C15 polyunsaturated side chain of cardanol through methoxylation has been shown to prevent the cross-linking processes to occur, the cardanol derivative only dimerizing under UV exposure but remaining fully soluble and thus appearing of tremendously lower photosensitivity as compared to cardanol. Incidentally, its photoaging mechanism – namely a dimerization through a phenol-phenol linkage – also highlights another photopolymerization process potentially

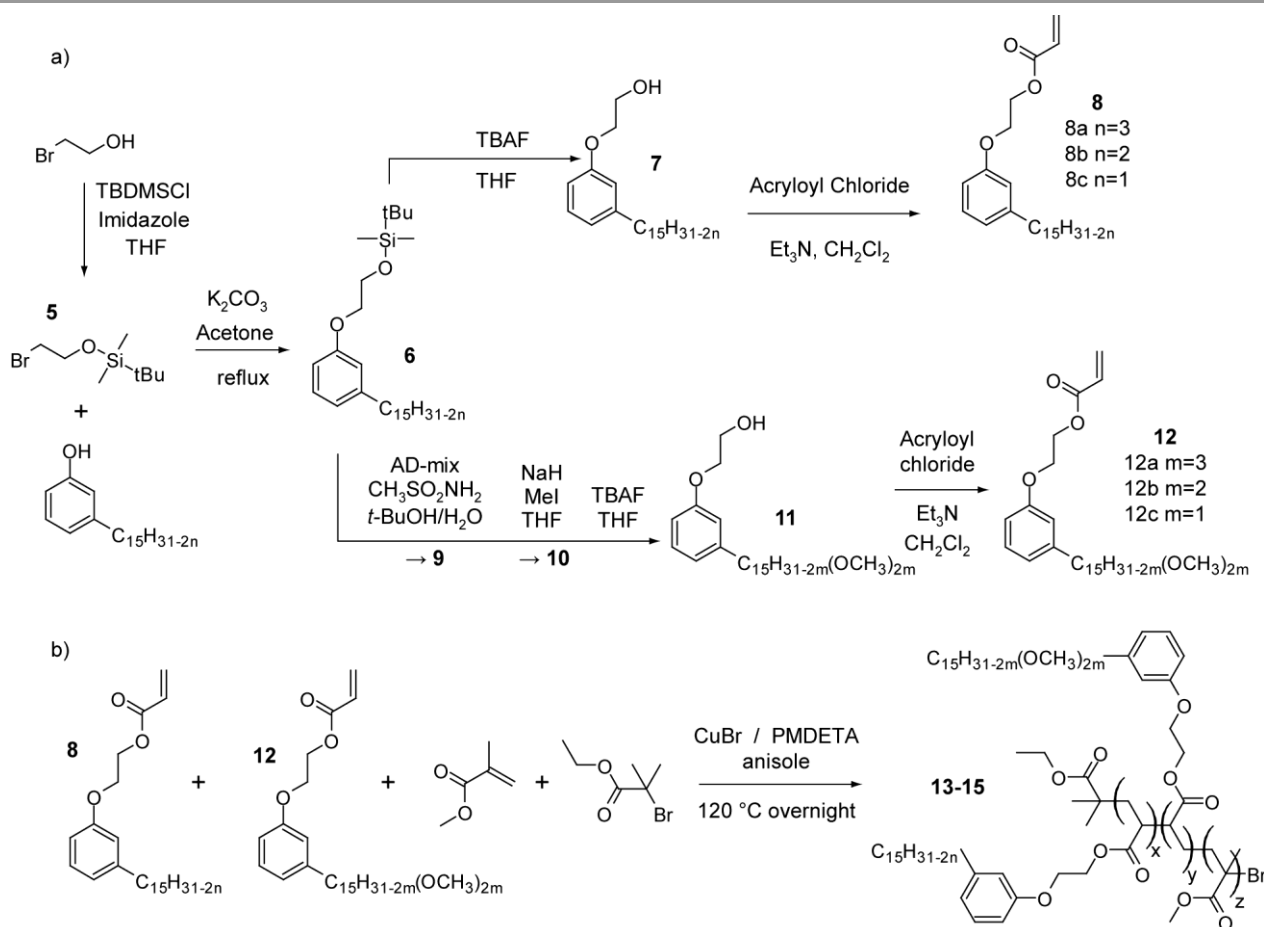
occurring for cardanol, which was not evidenced in the previous section owing to the predominance of the routes involving the side chains. By tailoring the structure of cardanol – a pristine side chain highly sensitive to UV photoaging or a methoxylated side chain which does not undergo severe modification – one could then expect to monitor the UV sensitivity of a cardanol-based product with a tunable *photocrosslinking* ability.

Cardanol-based copolymers of tunable photosensitivity

Acrylated monomers have been prepared with cardanol and methoxylated cardanol and subsequently copolymerized with MMA by ATRP, mimicking the structures proposed by Suresh et al.¹² Since the relative inertness of methoxylated cardanol has been observed in a timeframe cardanol would have turned into fully insoluble wax, it seems reasonable to expect a tunable propensity of copolymers whose co-monomeric composition has been properly monitored to photocrosslink under UV exposure. In the following section, poly(MMA-*r*-cardoxyethanol acrylate) (in lieu of acrylated cardanol) further noted poly(MMA-*r*-CEAcry), poly(MMA-*r*-methoxylated cardoxyethanol acrylate) noted poly(MMA-*r*-MCEAcry) and poly(MMA-*r*-methoxylated cardoxyethanol acrylate-*r*-cardoxyethanol acrylate) noted poly(MMA-*r*-MCEAcry-*r*-CEAcry) have been prepared and their UV sensitivity conveniently evaluated by SEC.

Synthesis of acrylated cardanol derivatives and copolymers

The synthesis routes followed to synthesize the so-called cardoxyethanol acrylate³⁷ and methoxylated cardoxyethanol acrylate are detailed in Scheme 2a (ESI† for the characterization of the cardoxyethanol acrylate **8** and the methoxylated cardoxyethanol **12**). In the ESI† is also briefly reported the characterization of a commercially available cardoxyethanol (**7** in Scheme 2a). Despite its use in lieu of cardanol would allow a one step shorter synthesis route, this industrial grade chemical contains nevertheless a large amount of oligomers and side products (ESI† for an unsuccessful attempt of purification) which would be deleterious for the functionalization and subsequent polymerization steps. Random copolymers were further synthesized by ATRP using MMA and **8** or MMA and **12** to produce copolymers noted **13** and **14**. A third terpolymer using MMA, **8** and **12** has finally been synthesized and noted **15**. Co-monomer ratios were targeted to 90:10, 90:10 and 90:5:5, respectively. Structures of the copolymers and the whole synthesis route are depicted in Scheme 2b.



Scheme 2. Synthesis routes to produce a) cardoxyethanol acrylate **8** and methoxylated cardoxyethanol acrylate **12** from cardanol and b) copolymers made of MMA and **8** 90/10 (noted **13**), MMA and **12** 90/10 (noted **14**), and a terpolymer from MMA, **8** and **12** 90/5/5 (noted **15**) by ATRP.

The SEC-MALDI(+)-MS and ¹H NMR spectra of the so-synthesized three copolymers **13-15** are depicted in Fig. 7. The SEC chromatograms recorded from a refractive index (RI) and UV/Vis detectors are depicted in insets in Fig. 7a-c. Note that the great similarities of peak shapes and retention times from RI and

UV ensure the (UV-active) cardanol moieties to be homogeneously distributed throughout the polymeric distribution, without any discrimination effect with regard to the MW. In all the three cases, a Gaussian-shaped polymeric distribution is readily detected in the SEC-MALDI(+)-MS

spectra. Their richness in terms of peaks is accounted for by considering that three components actually constitute the so-called cardoxyethanol acrylate **8** (+/- 2 Da, n=1-3) and methoxylated cardoxyethanol acrylate **12** (+/- 60 Da, m=1-3), making **13**, **14** and **15** to be formed of four, four and seven comonomers, respectively. The $^1\text{H-NMR}$ spectra of the copolymers/terpolymer are depicted in Fig. 7d-f. For **13**, aromatic ring and unsaturations from cardanol are highlighted by protons at $\delta=7$ ppm (noted **a**) and at $\delta=5.4$ ppm (noted **b**) while the methoxy groups from MMA are highlighted by protons at $\delta=3.6$ ppm and noted **c** (Fig. 7d). For **14**, aromatic ring and methoxy groups from *methoxylated* cardanol are highlighted by

protons noted **a** at $\delta=7$ ppm and **b'** at $\delta=3.4$ ppm, the methoxy groups from MMA are highlighted by protons **c** at $\delta=3.6$ ppm (Fig. 7e). The terpolymer structure of **15** is readily seen from the unsaturations of cardanol **b** and protons from the methoxy groups of methoxylated cardanol **b'** at $\delta=5.4$ ppm and $\delta=3.4$ ppm respectively (Fig. 7f) *i.e.* a combination of spectra of **13** and **14**.

Highlighting a tailored photosensitivity by SEC

Thin films of the three copolymers have been deposited on a glass substrate by drop casting ($\sim 6 \mu\text{m}$ measured by nanoscratch) and submitted to UV irradiation for 48h.

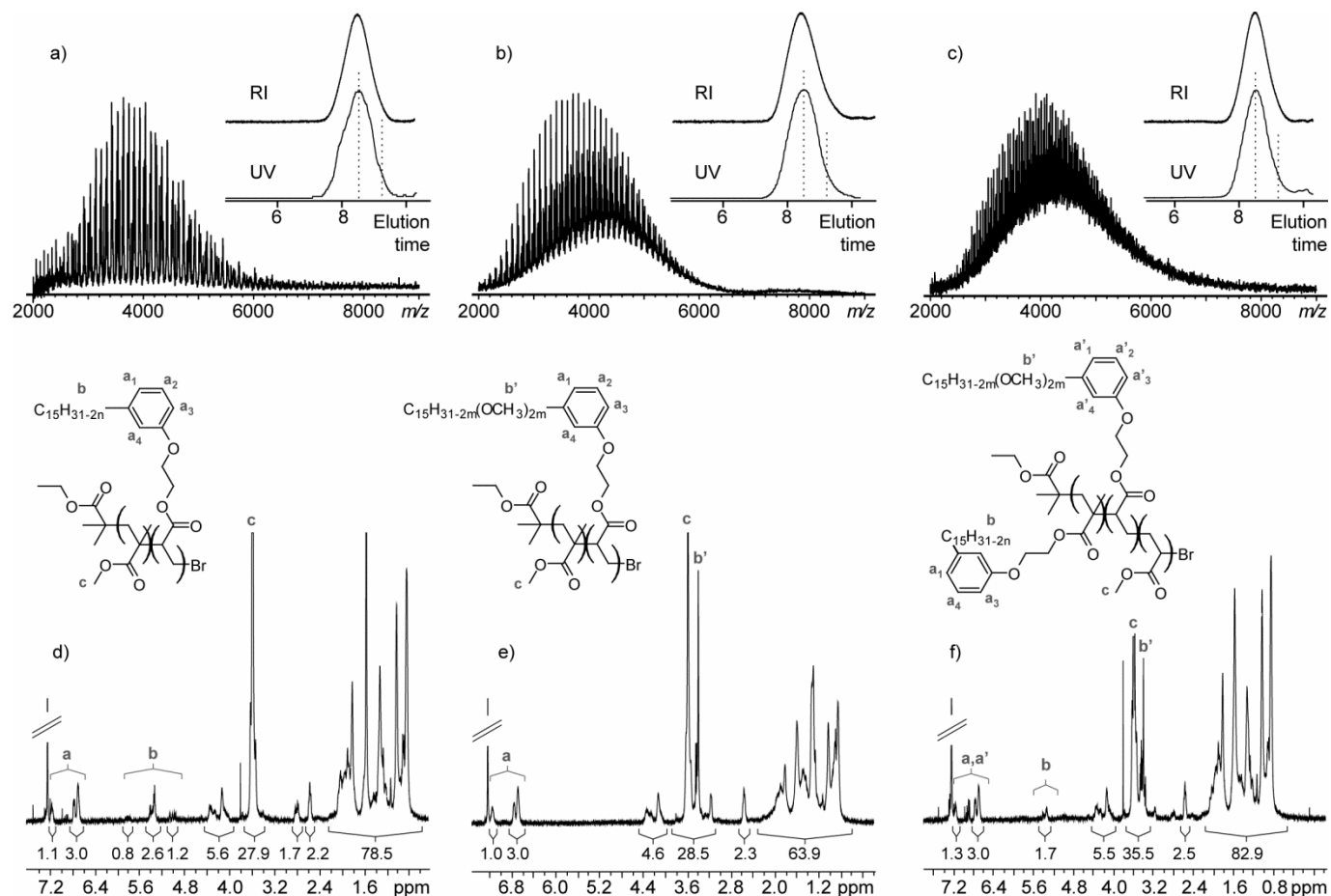


Fig. 7. SEC-MALDI(+)-MS spectra of the low molecular weight fractions from the SEC elutions of a) copolymer **13**, b) copolymer **14** and c) terpolymer **15**. SEC chromatograms recorded from RI and UV/Vis detectors are given in insets. d-f) $^1\text{H-NMR}$ spectra of the copolymers. Structures and assignments are given in insets.

Based on the previous results about the photosensitivity of cardanol and methoxylated cardanol, one should expect: a) copolymer **13** should undergo extensive crosslinking under UV as pristine cardanol, b) copolymer **14** should not undergo any modification in the timeframe of the experiment as methoxylated cardanol and c) terpolymer **15** should exhibit an intermediate behavior. After 48h, thin films were scrapped from the glass substrates and solubilized in THF. Both **13** and **15** were found not to fully solubilize but swell with solvent, while **14** fully dissolved in THF with no apparent residue. The SEC chromatograms recorded from the so-collected (soluble when

relevant) fractions are depicted in Fig. 8a-c (top) with the SEC chromatograms of the native copolymers for sake of comparison (bottom). In good agreement with the hypothesized behaviors, a very limited (<2 %) soluble part has been found for the cardanol-based copolymer **13**, giving rise to a nearly inexistent signal in UV detection (Fig. 8a). On the contrary, the methoxylated cardanol-based copolymer **14**, fully soluble, does not undergo any visible change in terms of molecular weight distribution, its SEC chromatogram remaining strictly similar to the pristine sample despite the photoaging (Fig. 8b). One should note that this inertness indirectly validates the dimerization process

through the phenol group (phenol-phenol coupling) proposed for methoxylated cardanol **4**. Indeed, the phenol group is naked in **4** but capped by a hydroxyethyl acrylate function in the MCEAcry co-monomer **12** and thus unavailable for dimerization. Finally, a soluble fraction evaluated at around 30% *w/w* has been collected from the terpolymer **15** (containing both cardanol and methoxylated cardanol), giving rise to a satisfactory SEC chromatogram but of lower relative abundance as compared to the pristine sample (Fig. 8c). In addition, a polymerization

process is clearly occurring and highlighted by a shouldering of the SEC peak towards the shorter elution times, *i.e.* the larger MW. SEC analyses clearly show a discrimination in the UV sensitivity of the three copolymers depending on their co-monomeric composition, in accordance with the respective sensitivity of cardanol and methoxylated cardanol from which the co-monomers have been derived. This preliminary result is of promising interest for the development of bio-based photo crosslinkable polymers with a tunable curing rate.

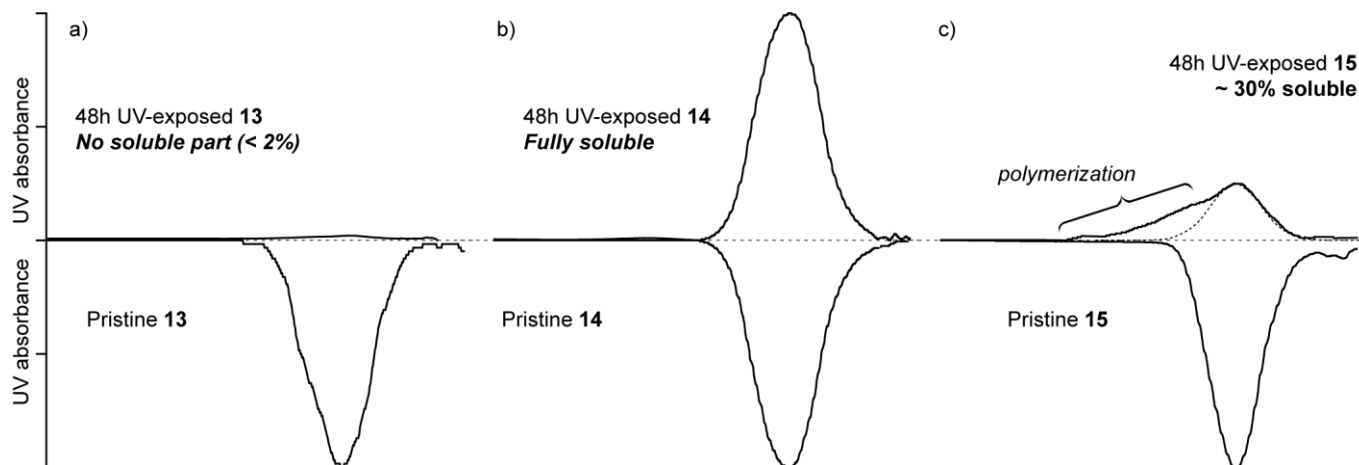


Fig. 8. SEC chromatograms of pristine copolymers / terpolymer (bottom) and after a 48h UV exposure (top, soluble parts when relevant). a) poly(MMA-r-CEAcry) **13**, b) poly(MMA-r-MCEAcry) **14** and c) poly(MMA-r-MCEAcry-r-CEAcry) **15**.

Conclusion

Through the implementation of several analytical techniques ranging from FTIR to SEC-MS coupling, the bare bones of the behavior of cardanol under UV exposure have been deciphered. In particular, oligomerization processes implicating its polyunsaturated side chain have been highlighted, ultimately leading to its complete insolubility in a short term. Such photosensitivity could appear as a fast ageing drawback but also and mainly as a promising photocrosslinking property. A functionalization of the side chain by methoxylation has been proposed and found to drastically limit the UV sensitivity of this newly synthesized cardanol derivative. In particular, cross linking reactions have been successfully avoided, despite some oxidative processes and a dimerization were still observed – none the less in a relative longer timeframe as compared to pristine cardanol. The combination of these two bio-based compounds has further permitted the preliminary monitoring of copolymers curing propensity under UV activation by tailoring their composition, as a promising step towards tunable photo crosslinkable bio based polymers.

Acknowledgements

Cardolite Specialty Chemical is gratefully acknowledged for the supply of cardanol used in this study.

Notes and references

Luxembourg Institute of Science and Technology (LIST), 5 avenue des Hauts-Fourneaux, 4362 Esch/Alzette (Luxembourg).

Emails: Thierry.fouquet@list.lu, ludivine.fetzer@list.lu

† Electronic Supplementary Information (ESI) available: [Structure of the cardanol components, UV/Vis spectra and SEC-UV/Vis spectra of UV-exposed cardanol, MALDI-MS spectra of intermediate products to the methoxylated cardanol, UV/Vis spectrum of UV-exposed methoxylated cardanol, MALDI-MS spectra of the CEAcry and MCEAcry monomers, SEC chromatograms, MALDI-MS spectra and SEC-MALDI-MS spectra of a commercially available cardoxyethanol]. See DOI: 10.1039/b000000x/

References

- 1 B. Lochab, S. Shukla, I.K. Varma, RSC Adv. 2014, 4, 21712-21752.
- 2 S. Kanehashi, K. Yokoyama, R. Masuda, T. Kidesaki, K. Nagai, T. Miyakoshi, J Appl. Polym. Sci. 2013, 130, 2468-2478.
- 3 T. de Jesus Aguiar dos Santos Andrade, B. Quirino Araújo, A. Maria das Graças Lopes Citó, J. da Silva, J. Saffi, M.F. Richter, A. de Barros Falcão Ferraz, Food Chem. 2011, 123, 1044-1048.
- 4 W. Arayaprane, G.L. Rempel, J. Appl. Polym. Sci. 2007, 106, 2696-2702.
- 5 G. Scott, Degradable Polymers: Principles and Applications, 2nd edition, Kluwer Academic Publishers, Dordrecht, 2003, pp 193-194.
- 6 V.S. Balachandran, S.R. Jadhav, P.K. Vemula, G. John, Chem. Soc. Rev. 2013, 42, 427-438.
- 7 C. Voirin, S. Caillol, N.V. Sadavarte, B.V. Tawade, B. Boutevin, P.P. Wadgaonkar, Polym. Chem. 2014, 5, 3142-3162.
- 8 S. Mohapatra, G.B. Nando, RSC Adv. 2014, 4, 15406-15418.

ARTICLE

- 9 S. Mohapatra, G.B. Nando, *Ind. Eng. Chem. Res.* 2013, 52, 5951–5957.
- 10 G. Mertz, Evolution des Propriétés physico-chimiques et mécaniques de composites à base caoutchouc lors du photo-vieillessement, PhD dissertation, 2011, pp. 24–27.
- 11 C. Adam, J. Lacoste, J. Lemaire, *Polym. Degrad. Stab.* 1989, 24, 185–200.
- 12 K.I. Suresh, M. Jaikrishna, *J. Polym. Sci. Pol. Chem.* 2005, 43, 5953–5961.
- 13 P. Verge, T. Fouquet, C. Barrère, V. Toniazzo, D. Ruch, J.A.S. Bomfim, *Compos. Sci. Technol.* 2013, 79, 126–132.
- 14 L. Puchot, P. Verge, T. Fouquet, J.A.S. Bomfim, V. Toniazzo, D. Ruch, *Appl. Clay Sci.* 2014, 99, 35–41.
- 15 M. Strohalm, D. Kavan, P. Novák, M. Volný, V. Havlíček, *Anal. Chem.* 2010, 82, 4648–4651.
- 16 S. Trimpin, A. Rouhanipour, R. Az, H.J. Räder, K. Müllen, *Rapid Commun. Mass Spectrom.* 2001, 15, 1364–1373.
- 17 S. Trimpin, S. Keune, H.J. Räder, K. Müllen, *J. Am. Soc. Mass Spectrom.* 2006, 17, 661–671.
- 18 S. Li, T. Zou, L. Feng, X. Liu, M. Tao, *J. Appl. Polym. Sci.* 2013, 128, 4164–4171.
- 19 D. Tiwari, A. Devi, R. Chandra, *Int. J. Drug Dev. & Res.* 2011, 3, 171–175.
- 20 M. Piton, A. Rivaton, *Polym. Degrad. Stab.* 1996, 53, 343–359.
- 21 L. Fertier, H. Koleilat, M. Stemmelen, O. Giani, C. Joly-Duhamel, V. Lapinte, J.-J. Robin, *Prog. Polym. Sci.* 2013, 38, 932–962.
- 22 M.T.S. Trevisan, B. Pfundstein, R. Haubner, G. Wurtele, B. Spiegelhalder, H. Bartsch, R.W. Owen, *Food Chem. Toxicol.* 2006, 44, 188–197.
- 23 P. Cesla, L. Blomberg, M. Hamberg, P. Jandera, *J. Chromatogr. A* 2006, 1115, 253–259.
- 24 R. Yadav, P. Awasthi, D. Srivastava, *J. Appl. Polym. Sci.* 2009, 114, 1471–1484.
- 25 T. Fouquet, L. Puchot, P. Verge, J.A.S. Bomfim, D. Ruch, *Anal. Chim. Acta* 2014, 843, 46–58.
- 26 H.C.M. Byrd, C.N. McEwen, *Anal. Chem.* 2000, 72, 4568–4576.
- 27 M.W.F. Nielen, S. Malucha, *Rapid Commun. Mass Spectrom.* 1997, 11, 1194–1204.
- 28 M.W.F. Nielen, *Mass Spectrom. Rev.* 1999, 18, 309–344.
- 29 M.S. Montaudo, C. Puglisi, F. Samperi, G. Montaudo, *Rapid Commun. Mass Spectrom.* 1998, 12, 519–528.
- 30 S.-I. Kuroda, A. Nagura, K. Horie, I. Mita, *Eur. Polym. J.* 1989, 25, 621–627.
- 31 S. Santeusano, O.A. Attanasi, R. Majer, M. Cangiotti, A. Fattori, M.F. Ottaviani, *Langmuir* 2013, 29, 11118–11126.
- 32 I.E. Bruce, A. Long, P.B. Payne, J.H. P. Tyman, *J. Liq. Chromatogr.* 1990, 13, 2103–2111.
- 33 T. Gandhi, M. Patel, B.K. Dholakiya, *J. Nat. Prod. Plant. Resour.* 2012, 2, 135–142.
- 34 K.I. Suresh, V.S. Kishanprasad, *Ind. Eng. Chem. Res.* 2005, 44, 4504–4512.
- 35 A.B. Dounay, G.J. Florence, A. Saito, C.J. Forsyth, *Tetrahedron* 2002, 58, 1865–1874.
- 36 J. Lachman, J. Dudjak, M. Orsák, V. Pivec, *Plant Soil Environ.* 2003, 49, 1–7.
- 37 K.I. Suresh, G. Foerst, R. Schubert, E. Bartsch, *J. Surfact. Deterg.* 2012, 15, 207–215.